

Stokes drag of spherical particles in a nematic environment at low Ericksen numbers

Holger Stark¹ and Dieter Venzki²¹Fachbereich Physik, Universität Konstanz, D-78457 Konstanz, Germany²Institut für Theoretische und Angewandte Physik, Universität Stuttgart, Pfaffenwaldring 57, D-70550 Stuttgart, Germany

(Received 1 March 2001; published 30 August 2001)

As a first approach to the motion of particles in anisotropic liquids, we study the Stokes drag of spherical particles in three different nematic environments: a uniform director field, the Saturn-ring configuration, and the dipole configuration. Two independent friction coefficients for the respective motion parallel and perpendicular to the overall symmetry axis exist. We determine these coefficients by solving the Ericksen-Leslie equations for low Ericksen numbers, i.e., when the director field is not influenced by the flow of the liquid crystal around the particle. We present streamline patterns and interpret them. Compared to the uniform director field and the Saturn-ring configuration, the dipolar configuration lacks a mirror plane as a symmetry element whose consequences we illustrate.

DOI: 10.1103/PhysRevE.64.031711

PACS number(s): 61.30.Dk, 47.50.+d, 83.10.-y, 61.30.Jf

I. INTRODUCTION

Particles in motion give rise to a wealth of interesting physics. For example, a common way to measure viscosities of liquids is the falling-ball method, where the velocity of the falling particle is determined by a balance of the gravitational, the buoyancy, and Stokes's friction force. Particles suspended in a fluid perform Brownian motion [1]. They are random walkers whose diffusion constant obeys the famous Stokes-Einstein relation [1]. A simple Langevin approach predicts that the velocity autocorrelation function of random walkers decays exponentially [1]. However, it displays a long-time tail due to the constant de- and acceleration of the particles [2–4]. Finally, particles moving relative to each other exchange shear waves, which leads to the so-called hydrodynamic interactions [1,5].

As a first approach to the motion of particles in anisotropic liquids, we study the Stokes drag of particles suspended in a nematic liquid crystal. In such liquids, rodlike organic molecules align, on average, along a common direction indicated by a unit vector \mathbf{n} called director. Stimulated by recent experiments on inverted nematic emulsions [6,7], there is a growing interest in suspensions of particles in a nematic environment [8–15]. A number of articles have addressed the director configuration around a single particle. They are reviewed in Ref. [16]. For rigid perpendicular anchoring of the molecules at the particle's surface and uniform director field at infinity, two configurations are found: (1) Together with a hyperbolic point defect in the director field, the particle forms a "rigid" dipole [see Fig. 1(1) and Refs. [6,11,12,17,18]]. (2) In the Saturn-ring configuration, a $-1/2$ disclination ring encircles the particle at its equator [see Fig. 1(2) and Refs. [9–12,17,18]]. If the anchoring strength of the director at the particle's surface is lowered, the disclination ring moves to the surface, and the surface-ring configuration occurs [10,12,17,18]. In the case of very weak anchoring, the particle is just floating in a uniform director field [see Fig. 1(3)]. All three configurations are observed in reality [6,7,19–21].

Early experiments in nematic liquid crystals measured the temperature and pressure dependence of an effective viscos-

ity η_{eff} in the Stokes drag [22,23]. Cladis *et al.* [22] argued that η_{eff} is close to the Mięsowicz shear viscosity η_b , i.e., to the case where the nematic fluid is flowing parallel to the director [24–27]. Nearly 20 years later, Poulin *et al.* used the Stokes drag to verify the dipolar force between two droplet-defect pairs in inverted nematic emulsions [28]. Böttger *et al.* observed the Brownian motion of particles above the nematic-isotropic phase transition [29]. Measuring the diffusion constant with the help of dynamic light scattering, they could show that, close to the phase transition, the effective viscosity in the Stokes drag increases due to surface-induced nematic order close to the particle.

A theoretical treatment of the Stokes drag has to deal with the dynamic equations of a nematic liquid crystal, i.e., the Ericksen-Leslie equations, which couple the director field and the fluid velocity. Due to their complexity, only few examples with an analytical solution exist, e.g., the flow between two parallel plates, which defines the different Mięsowicz viscosities [30], the Couette flow [31,32], the Poiseuille flow [33], which was first measured by Cladis *et al.* [22], or the back flow [34]. Besides the exploration of new effects, resulting from the coupling between the velocity and director field, solutions to the Ericksen-Leslie equations are also of technological interest since they are necessary for

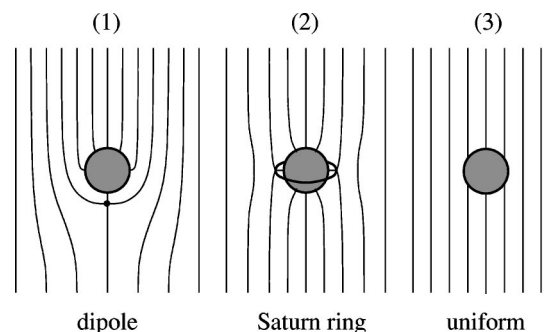


FIG. 1. Three possible director configurations for a spherical particle in a nematic environment with a uniform director field at infinity. The molecules are radially anchored at the surface of the particle. In configuration (3) a very weak surface anchoring is assumed.

determining the switching times of liquid-crystal displays.

The hydrodynamic solution for the flow of a nematic liquid crystal around a particle at rest, which is equivalent to the problem of a moving particle, presents another challenge to theorists. Diogo [35] assumed the velocity field to be the same as the one for an isotropic fluid and calculated the drag force for simple director configurations. He was interested in the case where the viscous forces largely exceed the elastic forces from director distortions, i.e., Ericksen numbers much larger than one, as we shall explain in the following section. Roman and Terentjev, concentrating on the opposite case, obtained an analytical solution for the flow velocity in a spatially uniform director field, by an expansion in the anisotropy of the viscosities [36]. Heuer *et al.* presented analytical and numerical solutions for both the velocity field and the Stokes drag, again assuming a uniform director field [37,38]. They were first investigating a cylinder of infinite length [39]. Ruhwandl and Terentjev allowed for a nonuniform but fixed director configuration, and they numerically calculated the velocity field and Stokes drag of a cylinder [40] or a spherical particle [41]. The particle was surrounded by the Saturn-ring configuration [see Fig. 1(2)], and the cylinder was accompanied by two disclination lines. Billeter and Pelcovits used molecular-dynamics simulations to determine the Stokes drag of very small particles [15]. They observed that the Saturn ring is strongly deformed due to the motion of the particles. Recently, Chono and Tsuji performed a numerical solution of the Ericksen-Leslie equations around a cylinder determining both the velocity and director field [42]. They could show that the director field strongly depends on the Ericksen number. However, for homeotropic anchoring, their director fields did not exhibit any topological defects required by the boundary conditions.

The Stokes drag of a particle surrounded by a disclination ring strongly depends on the presence of line defects. There exist a few studies, which determine both experimentally [43] and theoretically [44–46] the drag force of a moving disclination. In the multidomain cell, a novel liquid-crystal display, the occurrence of twist disclinations is forced by boundary conditions [47,48]. It is expected that the motion of these line defects strongly determines the switching time of the display.

The experiments on inverted nematic emulsions [6,28] and the investigations by Ruhwandl and Terentjev [41] motivated us to perform Stokes drag calculations for a particle in a nematic environment, especially for the particle-defect dipole [see Fig. 1(1)]. We concentrate on low Ericksen numbers, where the director field is not affected by the velocity field. We present streamline patterns, interpret them, calculate Stokes drags for motions parallel and perpendicular to the overall symmetry axis, and compare the results to the Saturn-ring configuration and a uniform director field. Compared to these systems, the dipole configuration lacks a mirror plane whose consequences we illustrate.

The paper is organized as follows. In Sec. II we discuss the theoretical concepts. We start with a short review of the Stokes drag in an isotropic fluid, introduce the Ericksen-Leslie equations, and formulate the limit of low Ericksen numbers, which reduces our problem considerably. A critical

remark about this limit ends the theory part. In Sec. III we explain the numerical method. Section IV presents our results and their discussion, and we finish with a conclusion in Sec. V.

II. THEORETICAL CONCEPTS

A. Stokes drag in an isotropic fluid

The Stokes drag in an isotropic fluid follows from a solution of the Navier-Stokes equations. Instead of considering a moving sphere, one solves the equivalent problem of the flow around a sphere at rest [49]. An incompressible fluid ($\text{div } \mathbf{v} = 0$) and a stationary velocity field ($\partial \mathbf{v} / \partial t = \mathbf{0}$) are assumed, so that the final set of equations reads

$$\text{div } \mathbf{v} = 0 \quad \text{and} \quad -\nabla p' + \text{div } \mathbf{T}' = \mathbf{0}. \quad (1)$$

In an isotropic fluid, the viscous stress tensor \mathbf{T}' is proportional to the symmetrized velocity gradient $A_{ij} = (\nabla_i v_j + \nabla_j v_i) / 2$, $\mathbf{T}' = 2 \eta \mathbf{A}$, where η denotes the usual shear viscosity. We have subdivided the pressure $p = p_0 + p'$ in a static (p_0) and a hydrodynamic (p') part. The static pressure only depends on the constant mass density ϱ and, therefore, does not appear in the momentum-balance equation of the set (1). The hydrodynamic contribution p' is a function of the velocity. It can be chosen zero at infinity. Furthermore, under the assumption of creeping flow, we have neglected the nonlinear velocity term in the momentum-balance equation resulting from the convective part of the total time derivative $d\mathbf{v}/dt = \partial \mathbf{v} / \partial t + \mathbf{v} \cdot \nabla \mathbf{v}$. That means, the ratio of inertial ($\varrho v^2 / a$) and viscous ($\eta v / a^2$) forces, which defines the *Reynolds number* $\text{Re} = \varrho v a / \eta$, is much smaller than one. To estimate the forces, all gradients are assumed to be of the order of the inverse particle radius a^{-1} , the characteristic length scale of our problem. Equations (1) are solved analytically for the nonslip condition at the surface of the particle [$\mathbf{v}(r=a) = \mathbf{0}$], and for a uniform velocity \mathbf{v}_∞ at infinity. Once the velocity and pressure fields are known, the drag force F_S follows from an integration of the total stress tensor $-\mathbf{p}\mathbf{1} + \mathbf{T}'$ over the particle surface. An alternative method demands that the dissipated energy per unit time, $\int (\mathbf{T}' \cdot \mathbf{A}) d^3r$, should be $F_S v_\infty$ [50]. The final result is the famous Stokes formula for the drag force:

$$F_S = \gamma v_\infty \quad \text{with} \quad \gamma = 6 \pi \eta a. \quad (2)$$

The symbol γ is called the friction coefficient. The Einstein-Stokes relation relates it to the diffusion constant D of a Brownian particle [51–53]: $D = k_B T / (6 \pi \eta a)$, where k_B is the Boltzmann constant and T is temperature.

We have also calculated the Stokes drag for a finite spherical region of radius $r = a/\varepsilon$ with the particle at its center. We followed the derivation for an infinite medium [49], however, assuming $p' = 0$ at $r = a/\varepsilon$. The result is

$$F_S = \gamma_\varepsilon v_\infty \quad \text{with} \quad \gamma_\varepsilon = 6 \pi \eta a \frac{1 - 3\varepsilon/2 + \varepsilon^3 - \varepsilon^5/2}{(1 - 3\varepsilon/2 + \varepsilon^3/2)^2}, \quad (3)$$

where we keep the notation v_∞ for the velocity at $r=a/\varepsilon$. The correction term is a monotonously increasing function in ε on the interesting interval $[0,1]$. Hence, the Stokes drag increases when the particle is confined to a finite volume. For $\varepsilon=1/32$, the correction is about 5%.

B. Ericksen-Leslie equations

To calculate the Stokes drag in a nematic environment, we have to deal with the Ericksen-Leslie equations, which couple the flow of the fluid to the director motion [26,27]. In a completely linearized form, they are identical to the hydrodynamic equations derived by the Harvard group [54,55]. Under the assumption of an incompressible fluid, stationary director and velocity fields, and $\text{Re} \ll 1$, the Ericksen-Leslie equations take the form

$$\text{div } \mathbf{v} = 0, \quad (4)$$

$$-\nabla p + \text{div}(\mathbf{T}^0 + \mathbf{T}') = \mathbf{0}, \quad (5)$$

$$\mathbf{n} \times (\mathbf{h}^0 - \mathbf{h}') = \mathbf{0}. \quad (6)$$

The divergence of the stress tensor is defined by $(\text{div } \mathbf{T})_i = \nabla_j T_{ij}$. Due to elastic distortions in the director field, an elastic stress tensor \mathbf{T}^0 occurs,

$$T_{ij}^0 = -\frac{\partial f_b}{\partial \nabla_j n_k} \nabla_i n_k, \quad (7)$$

where f_b stands for the Frank free-energy density [26,27]. In the one-constant approximation it reads $f_b = K(\nabla_i n_j)^2/2$. The uniaxial symmetry of the nematic liquid crystal allows for additional terms proportional to \mathbf{A} in the viscous stress tensor,

$$T'_{ij} = \alpha_1 n_i n_j n_k n_l A_{kl} + \alpha_2 n_j N_i + \alpha_3 n_i N_j + \alpha_4 A_{ij} + \alpha_5 n_j n_k A_{ik} + \alpha_6 n_i n_k A_{jk}. \quad (8)$$

The coefficients α_i are called Leslie viscosities. For different geometries, their combinations result in the three Mięslowicz shear viscosities [24–27]. In addition, a second dynamic variable

$$\mathbf{N} = \frac{\partial \mathbf{n}}{\partial t} + \mathbf{v} \cdot \nabla \mathbf{n} - \text{curl } \mathbf{v} \times \mathbf{n}/2, \quad (9)$$

appears. It describes the rate of change of \mathbf{n} relative to a fluid vortex. Note that in the stationary case ($\partial \mathbf{n} / \partial t = \mathbf{0}$) the convective derivative $\mathbf{v} \cdot \nabla \mathbf{n}$ is still present. It contributes whenever the fluid flows through a nonuniform, static director pattern as given, e.g., by the Saturn-ring and dipole configuration. Another famous example for this process is the Helfrich permeation for a static director helix [56].

The dynamic equation (6) balances elastic (\mathbf{h}^0) and viscous (\mathbf{h}') torques on the director,

$$h'_i = \nabla_j \frac{\partial f_b}{\partial \nabla_j n_i} - \frac{\partial f_b}{\partial n_i}, \quad (10)$$

$$h'_i = \gamma_1 N_i + \gamma_2 A_{ij} n_j. \quad (11)$$

The coefficient γ_1 is a true rotational viscosity for the director motion. As explained above, it contributes to the viscous torque even in the stationary case whenever $\nabla \mathbf{n} \neq \mathbf{0}$. Onsager relations require $\gamma_1 = \alpha_3 - \alpha_2$ and $\gamma_2 = \alpha_2 + \alpha_3$ [26,27].

C. Stokes drag in a nematic environment

In this paper we do not attempt to solve the Ericksen-Leslie equations in general. Instead, we will resort to an approximation already employed by Ruhwandl and Terentjev [40,41]. Analogous to the Reynolds number, we define the *Ericksen number* (Er) [45] as the ratio of viscous ($\eta v_\infty / a^2$) and elastic (K/a^3) forces in the momentum balance of Eq. (5):

$$\text{Er} = \frac{\eta v_\infty a}{K}. \quad (12)$$

The elastic forces are due to distortions in the director field, where K stands for an average Frank elastic constant. In the following, we assume $\text{Er} \ll 1$, i.e., the viscous forces are too weak to distort the director field, and we will always use the static director field for $\mathbf{v} = \mathbf{0}$ in our calculations. The condition $\text{Er} \ll 1$ constrains the velocity v_∞ . Using typical values of our parameters, i.e., $K = 10^{-6}$ dyn, $\eta = 0.1$ P, and $a = 10 \mu\text{m}$, we find

$$v_\infty \ll 100 \frac{\mu\text{m}}{\text{s}}. \quad (13)$$

Before we proceed, let us check for two cases if this constraint is fulfilled. First, via a phenomenological theory, one can show that the particle-defect dipoles interact like electric dipoles [6,11]. For inverted nematic emulsions, Poulin *et al.* invented a method to pull two water droplets apart [28]. When these droplets were released, they were approaching each other, with the Stokes drag balancing the dipolar force. By measuring the velocity as a function of droplet separation, the dipole interaction was verified. In these experiments the velocities of the particles were always smaller than $10 \mu\text{m/s}$. Second, in a falling-ball experiment, the velocity v of the falling particle is determined by a balance of the gravitational, the buoyancy, and Stokes's friction force, i.e., $6\pi\eta_{\text{eff}}av = (4\pi/3)a^3(\varrho - \varrho_{\text{n}})g$, and we obtain

$$v = \frac{2}{9} \frac{(\varrho - \varrho_{\text{n}})a^2g}{\eta_{\text{eff}}} \rightarrow 10^{-1} \frac{\mu\text{m}}{\text{s}}. \quad (14)$$

To arrive at the estimate, we choose $\eta_{\text{eff}} = 0.1$ P and $a = 10 \mu\text{m}$. We take $\varrho = 1 \text{ g/cm}^3$ as the mass density of the particle and $\varrho - \varrho_{\text{n}} = 0.01 \text{ g/cm}^3$ as its difference to the surrounding fluid [1].

After we have shown that $\text{Er} \ll 1$ is a reasonable assumption, we proceed as follows. We first calculate the static director field around a sphere from the balance of the elastic torques, $\mathbf{n} \times \mathbf{h}^0 = \mathbf{0}$ [see Eqs. (6) and (10)]. It corresponds to a minimization of the Frank free energy under the constraint that \mathbf{n} is a unit vector. For $\mathbf{v} = \mathbf{0}$, the static director field

defines a static pressure p_0 via the momentum balance, $-\nabla p_0 + \text{div } \mathbf{T}^0 = \mathbf{0}$ [see Eqs. (5) and (7)]. With the help of $\mathbf{n} \times \mathbf{h}^0 = \mathbf{0}$, one shows that $\text{div } \mathbf{T}^0 = -\nabla f_b$ [27]. Hence, the static pressure is known, $p_0 = \text{const} - f_b$. For $\mathbf{v} \neq \mathbf{0}$, we again divide the total pressure into its static and hydrodynamic part, $p = p_0 + p'$. Then the velocity field is determined from the same set of equations as in the isotropic case [see Eqs. (1)], provided that we employ the viscous stress tensor \mathbf{T}' of a nematic liquid crystal. In the case of an inhomogeneous director field, both the different Mięsowicz shear viscosities and the rotational viscosity γ_1 , discussed above, contribute to the Stokes drag.

In general, the friction force F_S does not point along \mathbf{v}_∞ , and the friction coefficient is now a tensor $\boldsymbol{\gamma}$. In the following, all our configurations are rotationally symmetric about the z axis, and the Stokes drag assumes the form

$$F_S = \boldsymbol{\gamma} \mathbf{v}_\infty \quad \text{with} \quad \boldsymbol{\gamma} = \gamma_\perp \mathbf{1} + (\gamma_\parallel - \gamma_\perp) \mathbf{e}_z \otimes \mathbf{e}_z. \quad (15)$$

The symbol \otimes means dyadic product and \mathbf{e}_z is a unit vector along the z direction. There only exist two independent components γ_\parallel and γ_\perp for a respective flow, parallel or perpendicular to the symmetry axis. In these two cases, the Stokes drag is parallel to \mathbf{v}_∞ . Otherwise, a component perpendicular to \mathbf{v}_∞ , called *lift force*, results [41]. In analogy with the isotropic fluid, we introduce effective viscosities $\eta_{\text{eff}}^\parallel$ and η_{eff}^\perp via

$$\gamma_\parallel = 6\pi \eta_{\text{eff}}^\parallel a \quad \text{and} \quad \gamma_\perp = 6\pi \eta_{\text{eff}}^\perp a. \quad (16)$$

It is sufficient to determine the velocity and pressure fields for two particular geometries with \mathbf{v}_∞ , either parallel or perpendicular to the z axis. Then, the friction coefficients are calculated with the help of the dissipated energy per unit time [27,35,41,50]:

$$F_S^{\parallel/\perp} \mathbf{v}_\infty = \int (\mathbf{T}' \cdot \mathbf{A} + \mathbf{h}' \cdot \mathbf{N}) d^3 r. \quad (17)$$

It turns out that the alternative method via an integration of the stress tensor at the surface of the particle is numerically less reliable. Note that the velocity and pressure fields for an arbitrary angle between \mathbf{v}_∞ and \mathbf{e}_z follow from superpositions of the solutions for the two selected geometries. This is due to the linearity of our equations in the velocity field \mathbf{v} .

It is clear that the Brownian motion in an environment with a rotational symmetry axis is governed again by two independent diffusion constants. The generalized Stokes-Einstein formula of the diffusion tensor \mathbf{D} takes the form

$$\mathbf{D} = D_\perp \mathbf{1} + (D_\parallel - D_\perp) \mathbf{e}_z \otimes \mathbf{e}_z, \quad D_{\parallel/\perp} = \frac{k_B T}{\gamma_{\parallel/\perp}}. \quad (18)$$

D. A critical remark

At the end, we add some critical remarks about our approach, which employs the static director field for $\mathbf{v} = \mathbf{0}$. From the balance equation of the elastic and viscous torques [see Eqs. (6), (10), and (11)], one derives that the change δn of the director due to the velocity \mathbf{v} is of the order of the

Ericksen number: $\delta n \sim \text{Er}$ [40]. This adds a correction $\delta \mathbf{T}^0$ to the elastic stress tensor \mathbf{T}^0 in the momentum balance equation that does not just renormalize the pressure. In the case of a spatially uniform director field, the correction $\delta \mathbf{T}^0$ is by a factor Er smaller than the viscous forces, and it can be neglected. However, for a nonuniform director field, it is of the same order as the viscous term, and, strictly speaking, should be taken into account. However by performing numerical calculations of the Stokes drag for arbitrary Ericksen numbers Er , we can show that the procedure, outlined here, is indeed valid for $\text{Er} \rightarrow 0$ [57]. We add two remarks that may help to clarify the problem. First, far away from the sphere, δn has to decay at least linearly in the $1/r$. Then one shows that $\delta \mathbf{T}^0$ is negligible against the viscous forces at least in the far field. Second, when calculating the isotropic Stokes drag, the nonlinear term $\mathbf{v} \cdot \nabla \mathbf{v}$ in the Navier-Stokes equations is usually omitted for $\text{Re} \ll 1$. However, whereas the friction and the pressure force for the Stokes problem decay as $1/r^3$, the nonlinear term is proportional to $1/r^2$, exceeding the first two terms in the far field. Nevertheless, performing extensive calculations, Oseen could prove that the correction of the nonlinear term to the Stokes drag is of the order of Re [49].

III. NUMERICAL METHOD

The numerical investigation is performed on a grid that is defined by modified spherical coordinates. Since the region outside the spherical particle is, in the extreme case, infinitely extended, we employ a reduced radial coordinate $\xi = a/r$. It maps the surface of the sphere ($r = a$) on $\xi = 1$ and $r = \infty$ on $\xi = 0$. The velocity and director fields are expressed in the local spherical coordinate basis $\{\mathbf{e}_r, \mathbf{e}_\theta, \mathbf{e}_\phi\}$ attached to each space point $\{\xi, \theta, \phi\}$:

$$\mathbf{n}(\mathbf{r}) = n_r \mathbf{e}_r + n_\theta \mathbf{e}_\theta, \quad (19)$$

$$\mathbf{v}(\mathbf{r}) = v_r \mathbf{e}_r + v_\theta \mathbf{e}_\theta + v_\phi \mathbf{e}_\phi. \quad (20)$$

The director field is restricted to a plane containing the rotational axis (z axis) of the director configurations in Fig. 1. We parametrized the director components with the help of the tilt angle Θ with respect to \mathbf{e}_r : $n_r = \cos \Theta$ and $n_\theta = \sin \Theta$. The director field was determined by minimizing the Frank free energy in the one-constant approximation numerically using the standard Newton-Gauss-Seidel method. The detailed procedure is described in Ref. [12].

To obtain the friction coefficient γ_\parallel , an effective two-dimensional problem has to be solved due to the rotational symmetry of the director configurations about the z axis. As for the director field, we set $v_\phi = 0$. In the case of γ_\perp ($\mathbf{v}_\infty \perp \mathbf{e}_z$), all three vector components of the velocity field have to be taken into account.

With our choice of modified spherical coordinates, the momentum balance of Eqs. (1) with the viscous stress tensor of a nematic [see Eq. (8)] becomes very complex in both the two- and three-dimensional cases. We, therefore, used the algebraic program MAPLE to calculate it. As input, the symmetrized gradient of the velocity field (\mathbf{A}), the rate of change of the director (\mathbf{N}), and the divergence of the viscous stress

tensor in spherical coordinates are needed, which we formulated with the help of standard methods from differential geometry. Since some of the formulas are hard to find in literature, we give the end results in the Appendix.

The two equations in Eq. (1) are treated by different numerical techniques. Given an initial velocity field, the momentum balance, including the inertial term $\partial \mathbf{v} / \partial t$, can be viewed as a relaxation equation towards the stationary velocity field, which we aim to determine. The Newton-Gauss-Seidel method [58] provides an effective tool to implement this relaxation. Employing the discretized version of the momentum balance equation, the velocity at the grid point \mathbf{r} relaxes according to

$$v_i^{\text{new}}(\mathbf{r}) = v_i^{\text{old}}(\mathbf{r}) - \frac{[-\nabla p' + \text{div } \mathbf{T}']_i}{[\partial(-\nabla p' + \text{div } \mathbf{T})]_i / \partial v_i(\mathbf{r})}. \quad (21)$$

Note that the denominator can be viewed as the inverse of a variable time step for the fictitious temporal dynamics of \mathbf{v} .

A relaxation equation for the pressure involving $\text{div } \mathbf{v} = 0$ is motivated by the method of artificial compressibility [59]. Let us consider the complete mass-balance equation. For small variations of the density, we obtain

$$\frac{\partial p}{\partial t} = -\frac{\varrho}{c^2} \text{div } \mathbf{v} \quad \text{with} \quad c = \sqrt{\frac{\partial p}{\partial \varrho}}. \quad (22)$$

The quantity c denotes the sound velocity for constant temperature, and c^2 / ϱ is the isothermal compressibility. In discretized form we have

$$p^{\text{new}} = p^{\text{old}} - \frac{\varrho}{c^2} \Delta t \text{div } \mathbf{v}. \quad (23)$$

Note that the reduced fictitious time step $\varrho \Delta t / c^2$ cannot be chosen according to the Newton-Gauss-Seidel method since $\text{div } \mathbf{v}$ does not contain the pressure p . Instead, it should be as large as possible to speed up the calculations. In Ref. [58] upper bounds are given beyond which the numerical scheme becomes unstable.

As already mentioned, to obtain the friction coefficient γ_{\parallel} , an effective two-dimensional problem has to be solved due to the rotational symmetry of the director configurations about the z axis. The integration area is defined by $0 \leq \theta \leq \pi$ and $\varepsilon \leq \xi \leq 1$, where we allow a finite extent of the region around the sphere. We assume the conventional non-slip boundary condition at the particle's surface and, in reduced units, $\mathbf{v}_{\infty} = \mathbf{e}_z$ at $\xi = \varepsilon$. In Table I all the boundary values are summarized. In the three-dimensional case of γ_{\perp} , we choose the velocity far away from the sphere as $\mathbf{v}_{\infty} = \mathbf{e}_x$. Then the velocity field possesses at least two mirror planes; the xz and the yz plane. As a result, the necessary three-dimensional calculations can be reduced to one quadrant of the real space ($0 \leq \phi \leq \pi/2$). The boundary values are described in Table II.

It turned out that the three-dimensional version of our programs is not completely stable for an infinitely extended integration volume. We therefore solved Eqs. (1) in a finite

TABLE I. Boundary values for the two-dimensional problem. The velocity at $\xi = \varepsilon$ is normalized to 1. Numbers are due to boundary conditions. The symbol sym means ‘‘required by symmetry.’’ The abbreviations linex and quadex stand, respectively, for ‘‘by linear’’ or ‘‘quadratic extrapolation.’’

	$\xi = \varepsilon$	$\xi = 1$	$\theta = 0$	$\theta = \pi$
v_r	$\cos \theta$	0	quadex	quadex
v_{θ}	$-\sin \theta$	0	sym \rightarrow 0	sym \rightarrow 0
p'	0	linex	quadex	quadex

region of reduced radius $r/a = 1/\varepsilon = 32$. For $\xi = \varepsilon = 1/32$, our programs reproduced the isotropic Stokes drag, calculated from Eq. (3), with an error smaller than 1%.

IV. RESULTS AND DISCUSSION

A. Streamline patterns

In Fig. 2 we compare the streamline patterns around a spherical particle for an isotropic liquid (right part, shaded light gray) and a spatially uniform director field parallel to \mathbf{v}_{∞} (left part). A uniform \mathbf{n} can be achieved by weak surface anchoring and application of a magnetic field with a magnetic coherence length smaller than the particle radius. In the isotropic fluid the bent stream lines occupy more space around the particle, whereas for a uniform director configuration they seem to follow the vertical director field lines as much as possible. This can be understood from a minimum principle. It is known that a shear flow along the director possesses the smallest of the three possible Mięsowicz shear viscosities [26,27], called η_b . Hence, in such a geometry, the smallest amount of energy is dissipated. Indeed, for a uniform director field, one can derive the momentum balance from a minimization of the dissipation function stated on the right-hand side of Eq. (17) [39]. A term $-2p \text{div } \mathbf{v}$ has to be added because of the incompressibility of the fluid. It turns out that the Lagrange multiplier $-2p$ is determined by the pressure p .

In the case of the topological dipole parallel to \mathbf{v}_{∞} , we observe a clear asymmetry in the streamlines as illustrated in Fig. 3. The dot indicates the position of the point defect. It breaks the mirror symmetry of the streamline pattern, which exists, e.g., in an isotropic liquid relative to a plane perpendicular to the vertical axis. In the far field of the velocity, the splay deformation in the dipolar director configuration is clearly recognizable. Since we use the linearized momentum balance in \mathbf{v} , the velocity field is the same no matter if the fluid flows upward or downward. The streamline pattern of the Saturn ring [see Fig. 4 (right, shaded light gray)] exhibits the mirror symmetry, and the position of the ring disclination is visible by a dip in the streamline close to the equator of the sphere.

If \mathbf{v}_{∞} is perpendicular to the dipole axis, the missing mirror plane of the dipole configuration is even more pronounced in the streamline pattern. It is illustrated in Fig. 5, where the point defect is indicated by a dip in the streamline. Although the pattern resembles the one of the Magnus effect

TABLE II. Boundary values for the three-dimensional problem. The velocity at $\xi = \varepsilon$ is normalized to 1. Numbers are due to boundary conditions. The symbol sym means “required by symmetry.” The abbreviations linex and quadex stand, respectively, for by “linear” or “quadratic extrapolation.” On the z axis ($\theta = 0, \pi$), we determine v_θ by quadratic extrapolation. Then v_ϕ is fixed since, by symmetry, the velocity has to point along the x axis.

	$\xi = \varepsilon$	$\xi = 1$	$\theta = 0$	$\theta = \pi$	$\phi = 0$	$\phi = \pi/2$
v_r	$\sin \theta \cos \phi$	0	sym \rightarrow 0	sym \rightarrow 0	quadex	sym \rightarrow 0
v_θ	$\cos \theta \cos \phi$	0	quadex	quadex	quadex	sym \rightarrow 0
v_ϕ	$-\sin \phi$	0	sym	sym	sym \rightarrow 0	quadex
p'	0	linex	sym \rightarrow 0	sym \rightarrow 0	quadex	0

[49], symmetry dictates that $F_S^\perp \parallel \mathbf{v}_\infty$. A lift force, perpendicular to \mathbf{v}_∞ , does not exist. However, we find a nonzero viscous torque acting on the particle whose direction for a fluid flow from left to right is indicated in Fig. 5. Symmetry allows such a torque \mathbf{M} since the cross product of a dipole moment \mathbf{p} , which can be assigned to the dipolar configuration (see Refs. [6,11]), and \mathbf{v}_∞ gives an axial or pseudovector $\mathbf{M} \propto \mathbf{p} \times \mathbf{v}_\infty$. In the Saturn-ring configuration, a nonzero dipole moment does not exist by symmetry. Therefore, a nonzero torque cannot occur.

B. Effective viscosities

In Table III we summarize the effective viscosities of the Stokes drag, defined in Eq. (16), for a uniform director field, the dipole, and the Saturn-ring configuration. The values are calculated for the two compounds MBBA and 5CB. As a reference, we include the three Mięslowicz viscosities. In the case of \mathbf{v}_∞ parallel to the symmetry axis of the three configurations, we might expect that $\eta_{\text{eff}}^\parallel$ is close to η_b as argued by Cladis *et al.* [22]. For a uniform director field, $\eta_{\text{eff}}^\parallel$ exceeds η_b by 30% or 60%, respectively. The increase originates in the streamlines bending around the particle. The effective viscosity $\eta_{\text{eff}}^\parallel$ of the dipole and the Saturn ring are larger than η_b by an approximate factor of 2. In addition to the bent stream lines, there exist strong director distortions close to the particle that the fluid has to flow through, constantly changing the local direction of the moving molecules.

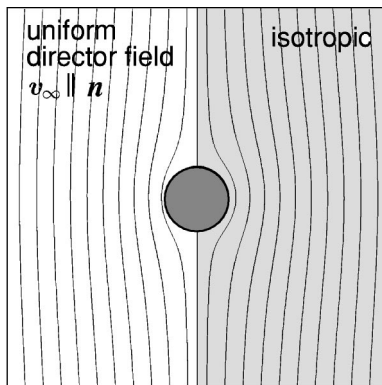


FIG. 2. Streamline pattern around a spherical particle for an isotropic liquid (right, shaded light gray) and a uniform director field parallel to \mathbf{v}_∞ (left).

Recalling our note in Sec. II B following Eq. (9), a contribution from the rotational viscosity γ_1 arises, which does not exist in a uniform director field. In all three cases, we find $\eta_{\text{eff}}^\parallel$ either close to or larger than η_a . The Mięslowicz viscosity η_a determines a shear flow with the uniform director field perpendicular to the velocity gradient. So it is obvious that η_b is not the only determining quantity of $\eta_{\text{eff}}^\parallel$, as argued by Cladis *et al.* [22]. For \mathbf{v}_∞ perpendicular to the symmetry axis, η_{eff}^\perp assumes a value between η_a and η_c . This observation is understandable since the Mięslowicz viscosity η_c determines a shear flow with the director perpendicular to the velocity, which is mainly the case in our second geometry.

The ratio $\eta_{\text{eff}}^\perp / \eta_{\text{eff}}^\parallel$ for the uniform director field is the largest since the extreme cases of a respective flow, parallel or perpendicular to the director field, is realized the best in this configuration. Furthermore, both the dipole and the Saturn ring exhibit nearly the same anisotropy, and we conclude that they cannot be distinguished from each other in a falling-ball experiment. The ratios $\eta_{\text{eff}}^\perp / \eta_{\text{eff}}^\parallel$, which we determine for the Saturn ring and the uniform director field in the case of the compound MBBA, agree well with the results of Ruhwandl and Terentjev who find $\eta_{\text{eff}}^\perp / \eta_{\text{eff}}^\parallel |_{\text{uniform}} = 1.69$ and $\eta_{\text{eff}}^\perp / \eta_{\text{eff}}^\parallel |_{\text{Saturn}} = 1.5$ [41]. However, they differ from the findings of Billeter and Pelcovits in their molecular-dynamics simulations [15].

We have also performed calculations where we replaced the numerically determined director fields by ansatz functions that are very close to the numerical fields [11,12]. In the

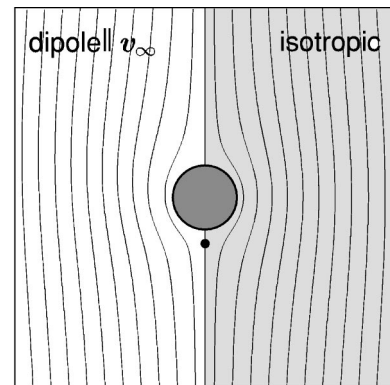


FIG. 3. Streamline pattern around a spherical particle for an isotropic liquid (right, shaded light gray) and the topological dipole parallel to \mathbf{v}_∞ (left).

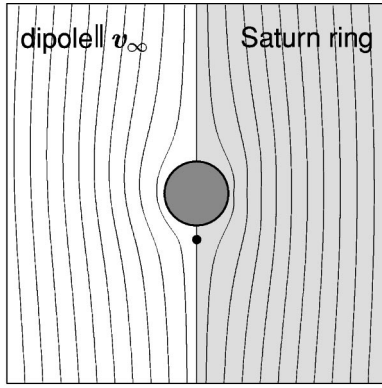


FIG. 4. Streamline pattern around a spherical particle for the Saturn ring (right, shaded light gray) and the topological dipole (left) with their respective symmetry axis parallel to \mathbf{v}_∞ .

ansatz function of the dipolar configuration, we vary the separation r_d between the hedgehog and the center of the particle. Both the effective viscosities increase with r_d since the nonuniform director field with its strong distortions occupies more space. However, the ratio $\eta_{\text{eff}}^\perp/\eta_{\text{eff}}^\parallel$ basically remains the same. For the Saturn ring, $\eta_{\text{eff}}^\parallel$ increases stronger with the radius r_d than does η_{eff}^\perp . This seems to be reasonable since a flow perpendicular to the plane of the Saturn ring experiences more resistance than a flow parallel to the plane. As a result, $\eta_{\text{eff}}^\perp/\eta_{\text{eff}}^\parallel$ decreases when the ring radius r_d is enlarged.

V. CONCLUSIONS

We have studied the Stokes drag of a spherical particle in three different nematic environments: a uniform director field, the Saturn-ring, and the dipole configuration. We have presented streamline patterns of the velocity. In the uniform director field, the streamlines follow as much as possible the director field lines, which we explained by minimization of the dissipated energy. The dipole lacks a mirror plane perpendicular to its rotational axis. The consequences are clearly seen in the streamline patterns. Furthermore, for \mathbf{v}_∞ perpendicular to the symmetry axis, a nonzero viscous torque is possible that cannot appear in the two other configurations. We have calculated effective viscosities for the two main directions of the Stokes drag, and we have pointed out the role of the rotational viscosity γ_1 in the Ericksen-Leslie equations. Interestingly, the ratio $\eta_{\text{eff}}^\perp/\eta_{\text{eff}}^\parallel$ is nearly the same in the dipole and the Saturn-ring configuration so that they cannot be distinguished by measuring the Stokes drag.

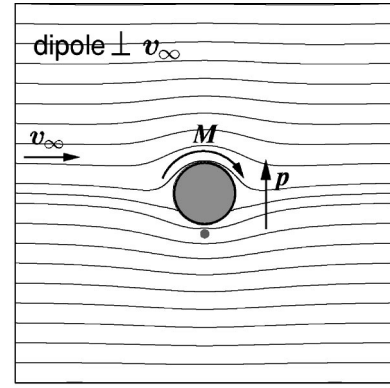


FIG. 5. Streamline pattern around a spherical particle for the topological dipole perpendicular to \mathbf{v}_∞ .

We have started to perform a complete solution of the Ericksen-Leslie equations including a relaxation of the static director field for $\mathbf{v} \neq \mathbf{0}$. Such calculations help to gain insight into several open problems. First, there was the question if the corrections to the Stokes drag are of the order of Er . Results for the two-dimensional problem with the relaxation of the director field included show that the Stokes drag of the dipolar configuration varies indeed linearly in Er for $\text{Er} < 1$. Furthermore, it is highly nonlinear depending on \mathbf{v}_∞ being either parallel or antiparallel to the topological dipole. Details of these investigations will be published elsewhere [57]. A second problem concerns the orientation of the dipole. For $\text{Er} \rightarrow 0$, the Stokes drag of the topological dipole is the same, whether the flow is parallel or antiparallel to the dipole moment. This is also true for an object with a dipolar shape in an isotropic fluid. If such an object is slightly turned away from its orientation parallel to \mathbf{v}_∞ , it will experience a viscous torque and either relax back or reverse its direction to find its absolute stable orientation. The topological dipole will not turn around since it experiences an elastic torque towards its initial direction that is fixed by the director field at infinity [11]. Nevertheless, a full solution of the Ericksen-Leslie equations would show whether and how much the dipole deviates from its preferred direction under the influence of a velocity field. It would also clarify its orientation when \mathbf{v}_∞ is perpendicular to the dipolar axis. At last, there is the nonzero viscous torque in the three-dimensional geometry. We speculate that it is cancelled by elastic torques if a full solution of the Ericksen-Leslie equations is performed.

The Stokes drag of particles in a nematic environment still presents a challenging problem to theorists. On the other

TABLE III. Effective viscosities of the Stokes drag for the two compounds MBBA and 5CB and for three different director configurations. As a reference, the three Mięsowicz viscosities are included.

	MBBA			5CB		
	$\eta_a=0.416$ P, Uniform \mathbf{n}	$\eta_b=0.283$ P, Dipole	$\eta_c=1.035$ P Saturn ring	$\eta_a=0.374$ P, Uniform \mathbf{n}	$\eta_b=0.229$ P, Dipole	$\eta_c=1.296$ P Saturn ring
$\eta_{\text{eff}}^\parallel$ [P]	0.371	0.503	0.485	0.375	0.525	0.494
η_{eff}^\perp [P]	0.687	0.770	0.755	0.751	0.864	0.853
$\eta_{\text{eff}}^\perp/\eta_{\text{eff}}^\parallel$	1.85	1.53	1.56	2.00	1.64	1.72

hand, clear measurements of, e.g., the anisotropy in Stokes's friction force are missing.

ACKNOWLEDGMENTS

The authors thank T. C. Lubensky, P. Palffy-Muhoray, A. Rüdinger, J. Stelzer, E. M. Terentjev, and H.-R. Trebin for helpful discussions. The work was supported by the Deutsche Forschungsgemeinschaft under Grant Nos. Tr 154/17-1/2 and Sta 352/5-1.

APPENDIX

For our numerical treatment, the set of Eqs. (1) has to be formulated in spherical coordinates. For completeness, we give the divergence of the velocity field:

$$\operatorname{div} \mathbf{v} = \frac{\partial v_r}{\partial r} + \frac{2v_r}{r} + \frac{1}{r} \frac{\partial v_\theta}{\partial \theta} + \frac{\cot \theta}{r} v_\theta + \frac{1}{r \sin \theta} v_\phi. \quad (\text{A1})$$

The formula for the viscous stress tensor of Eq. (8) is also valid in spherical coordinates with all components chosen relative to the spherical coordinate basis $(i, j, k, l = r, \theta, \phi)$. The symmetrized velocity gradient \mathbf{A} is derived from the gradient of the velocity field:

$\operatorname{grad} \mathbf{v}$

$$= \begin{pmatrix} \frac{\partial v_r}{\partial r} & \frac{1}{r} \frac{\partial v_r}{\partial \theta} - \frac{v_\theta}{r} & \frac{1}{r \sin \theta} \frac{\partial v_r}{\partial \phi} - \frac{v_\phi}{r} \\ \frac{\partial v_\theta}{\partial r} & \frac{1}{r} \frac{\partial v_\theta}{\partial \theta} + \frac{v_r}{r} & \frac{1}{r \sin \theta} \frac{\partial v_\theta}{\partial \phi} - \frac{\cot \theta}{r} v_\phi \\ \frac{\partial v_\phi}{\partial r} & \frac{1}{r} \frac{\partial v_\phi}{\partial \theta} & \frac{1}{r \sin \theta} \frac{\partial v_\phi}{\partial \phi} + \frac{v_r}{r} + \frac{\cot \theta}{r} v_\theta \end{pmatrix}. \quad (\text{A2})$$

The dynamic variable N [see Eq. (9)] involves the curl of the velocity field:

$$\operatorname{curl} \mathbf{v} = \left(\frac{1}{r} \frac{\partial v_\phi}{\partial \theta} + \frac{\cot \theta}{r} v_\phi - \frac{1}{r \sin \theta} \frac{\partial v_\theta}{\partial \phi} \right) \mathbf{e}_r + \left(\frac{1}{r \sin \theta} \frac{\partial v_r}{\partial \phi} - \frac{\partial v_\phi}{\partial r} - \frac{v_\phi}{r} \right) \mathbf{e}_\theta + \left(\frac{\partial v_\theta}{\partial r} + \frac{v_\theta}{r} - \frac{1}{r} \frac{\partial v_r}{\partial \theta} \right) \mathbf{e}_\phi, \quad (\text{A3})$$

from which the cross product with the director field \mathbf{n} is readily calculated. The convective term in N contains the gradient of \mathbf{n} which is analogous to Eq. (A2). It is contracted with \mathbf{v} . The viscous stress tensor can now be formulated. We need its divergence that is a vector with the following components:

$$(\operatorname{div} \mathbf{T}')_r = \frac{\partial T_{rr}}{\partial r} + \frac{2}{r} T_{rr} + \frac{1}{r} \frac{\partial T_{r\theta}}{\partial \theta} + \frac{\cot \theta}{r} T_{r\theta} + \frac{1}{r \sin \theta} \frac{\partial T_{r\phi}}{\partial \phi} - \frac{1}{r} T_{\theta\theta} - \frac{1}{r} T_{\phi\phi}, \quad (\text{A4})$$

$$(\operatorname{div} \mathbf{T}')_\theta = \frac{1}{r} T_{r\theta} + \frac{\partial T_{\theta r}}{\partial r} + \frac{2}{r} T_{\theta r} + \frac{1}{r} \frac{\partial T_{\theta\theta}}{\partial \theta} + \frac{\cot \theta}{r} T_{\theta\theta} + \frac{1}{r \sin \theta} \frac{\partial T_{\theta\phi}}{\partial \phi} - \frac{\cot \theta}{r} T_{\phi\phi}, \quad (\text{A5})$$

$$(\operatorname{div} \mathbf{T}')_\phi = \frac{1}{r} T_{r\phi} + \frac{\partial T_{\phi r}}{\partial r} + \frac{2}{r} T_{\phi r} + \frac{\cot \theta}{r} (T_{\theta\phi} + T_{\phi\theta}) + \frac{1}{r} \frac{\partial T_{\phi\theta}}{\partial \theta} + \frac{1}{r \sin \theta} \frac{\partial T_{\phi\phi}}{\partial \phi}. \quad (\text{A6})$$

Finally, the differential operators for our modified spherical coordinates result from the substitution

$$r = 1/\xi \quad \text{and} \quad \frac{\partial}{\partial r} = -\xi^2 \frac{\partial}{\partial \xi}. \quad (\text{A7})$$

In using the operators, one has to remember that the director configurations are axially symmetric about the z axis, i.e., they do not depend on the azimuthal angle ϕ , and that the azimuthal component is zero: $n_\phi = 0$. In the two-dimensional calculation to determine γ_{\parallel} , the same holds for the velocity field.

-
- [1] W.B. Russel, D.A. Saville, and W.R. Schowalter, *Colloidal Dispersions* (Cambridge University Press, Cambridge, UK, 1995).
- [2] B.J. Alder and T.E. Wainwright, Phys. Rev. Lett. **18**, 988 (1976).
- [3] B.J. Alder and T.E. Wainwright, J. Phys. Soc. Jpn. **26**, 267 (1969).
- [4] B.J. Alder and T.E. Wainwright, Phys. Rev. A **1**, 18 (1970).
- [5] R. Klein, in *The Physics of Complex Systems*, edited by F. Mallamace and H.E. Stanley (IOS, Amsterdam, 1997), pp. 301–345.
- [6] P. Poulin, H. Stark, T.C. Lubensky, and D.A. Weitz, Science **275**, 1770 (1997).
- [7] P. Poulin and D.A. Weitz, Phys. Rev. E **57**, 626 (1998).
- [8] P. Poulin, V.A. Raghunathan, P. Richetti, and D. Roux, J. Phys. II **4**, 1557 (1994).
- [9] E.M. Terentjev, Phys. Rev. E **51**, 1330 (1995).
- [10] O.V. Kuksenok, R.W. Ruhwandl, S.V. Shiyanovskii, and E.M. Terentjev, Phys. Rev. E **54**, 5198 (1996).
- [11] T.C. Lubensky, D. Petey, N. Currier, and H. Stark, Phys. Rev.

- E **57**, 610 (1998).
- [12] H. Stark, *Eur. Phys. J. B* **10**, 311 (1999).
- [13] S.P. Meeker, W.C.K. Poon, J. Crain, and E.M. Terentjev, *Phys. Rev. E* **61**, R6083 (2000).
- [14] J.-C. Loudet, P. Barois, and P. Poulin, *Nature (London)* **407**, 611 (2000).
- [15] J.L. Billeter and R.A. Pelcovits, *Phys. Rev. E* **62**, 711 (2000).
- [16] H. Stark, *Phys. Rep.* (to be published).
- [17] R.W. Ruhwandl and E.M. Terentjev, *Phys. Rev. E* **56**, 5561 (1997).
- [18] S.V. Shiyonovskii and O.V. Kuksenok, *Mol. Cryst. Liq. Cryst.* **321**, 45 (1998).
- [19] P. Poulin, N. Francès, and O. Mondain-Monval, *Phys. Rev. E* **59**, 4384 (1999).
- [20] Y. Gu and N.L. Abbott, *Phys. Rev. Lett.* **85**, 4719 (2000).
- [21] O. Mondain-Monval, J.C. Dedieu, T. Gulik-Krzywicki, and P. Poulin, *Eur. Phys. J. B* **12**, 167 (1999).
- [22] A.E. White, P.E. Cladis, and S. Torza, *Mol. Cryst. Liq. Cryst.* **43**, 13 (1977).
- [23] E. Kuss, *Mol. Cryst. Liq. Cryst.* **47**, 71 (1978).
- [24] M. Mięslowicz, *Nature (London)* **136**, 261 (1935).
- [25] M. Mięslowicz, *Nature (London)* **158**, 27 (1946).
- [26] S. Chandrasekhar, *Liquid Crystals*, 2nd ed. (Cambridge University Press, Cambridge, UK, 1992).
- [27] P.G. de Gennes and J. Prost, *The Physics of Liquid Crystals*, 2nd ed. (Oxford Science, Oxford, 1993).
- [28] P. Poulin, V. Cabuil, and D.A. Weitz, *Phys. Rev. Lett.* **79**, 4862 (1997).
- [29] A. Böttger, D. Frenkel, E. van de Riet, and R. Zijlstra, *Mol. Cryst. Liq. Cryst.* **2**, 539 (1987).
- [30] P.K. Currie, *J. Phys. (France)* **40**, 501 (1979).
- [31] R.J. Atkin and F.M. Leslie, *Q. J. Mech. Appl. Math.* **23**, S3 (1970).
- [32] P.K. Currie, *Arch. Ration. Mech. Anal.* **37**, 222 (1970).
- [33] R.J. Atkin, *Arch. Ration. Mech. Anal.* **38**, 224 (1970).
- [34] P. Pieranski, F. Brochard, and E. Guyon, *J. Phys. (France)* **34**, 35 (1973).
- [35] A.C. Diogo, *Mol. Cryst. Liq. Cryst.* **100**, 153 (1983).
- [36] V.G. Roman and E.M. Terentjev, *Colloid J. USSR* **51**, 435 (1989).
- [37] H. Kneppé, F. Schneider, and B. Schwesinger, *Mol. Cryst. Liq. Cryst.* **205**, 9 (1991).
- [38] H. Heuer, H. Kneppé, and F. Schneider, *Mol. Cryst. Liq. Cryst.* **214**, 43 (1992).
- [39] H. Heuer, H. Kneppé, and F. Schneider, *Mol. Cryst. Liq. Cryst.* **200**, 70 (1991).
- [40] R.W. Ruhwandl and E.M. Terentjev, *Z. Naturforsch. Teil A* **50**, 1023 (1995).
- [41] R.W. Ruhwandl and E.M. Terentjev, *Phys. Rev. E* **54**, 5204 (1996).
- [42] S. Chono and T. Tsuji, *Mol. Cryst. Liq. Cryst.* **309**, 217 (1998).
- [43] P.E. Cladis, W. van Saarloos, P.L. Finn, and A.R. Kortan, *Phys. Rev. Lett.* **58**, 222 (1987).
- [44] H. Imura and K. Okano, *Phys. Lett. A* **42**, 403 (1973).
- [45] P.G. de Gennes, in *Molecular Fluids*, edited by R. Balian and G. Weill (Gordon and Breach, London, 1976), pp. 373–400.
- [46] G. Ryskin and M. Kremenetsky, *Phys. Rev. Lett.* **67**, 1574 (1991).
- [47] M. Schadt, H. Seiberle, and A. Schuster, *Nature (London)* **318**, 212 (1996).
- [48] M. Reichenstein, T. Seitz, and H.-R. Trebin, *Mol. Cryst. Liq. Cryst.* **330**, 549 (1999).
- [49] A. Sommerfeld, *Vorlesungen über Theoretische Physik II. Mechanik der deformierbaren Medien*, 6th ed. (Verlag Harri Deutsch, Frankfurt, 1978).
- [50] R.B. Bird, W.E. Stewart, and E.N. Lightfoot, *Transport Phenomena* (Wiley, New York, 1960).
- [51] A. Einstein, *Ann. Phys. (Leipzig)* **17**, 549 (1905).
- [52] A. Einstein, *Ann. Phys. (Leipzig)* **19**, 289 (1906).
- [53] A. Einstein, *Ann. Phys. (Leipzig)* **19**, 371 (1906).
- [54] D. Forster, *Hydrodynamic Fluctuations, Broken Symmetry, and Correlation Functions* (Benjamin, Reading, MA, 1975).
- [55] P. Chaikin and T.C. Lubensky, *Principles of Condensed Matter Physics* (Cambridge University Press, Cambridge, UK, 1995).
- [56] W. Helfrich, *Phys. Rev. Lett.* **23**, 372 (1969).
- [57] H. Stark and D. Venzki, *Europhys. Lett.* (to be published).
- [58] W.H. Press, S.A. Teukolsky, W.T. Vetterling, and B.P. Flannery, *Numerical Recipes in Fortran: The Art of Scientific Computing* (Cambridge University Press, Cambridge, UK, 1992).
- [59] A.J. Chorin, *J. Comput. Phys.* **2**, 12 (1967).